



Effect of high-throughput screening of circRNA01724 on a rat model of myocardial ischemia ventricular arrhythmia

Xiaomin Hu^{1#}, Dan Wu^{2#}, Bing Zou³, Huiling Xiao¹, Tao Yang³, Chenxi Wang¹, Hui Zhou¹, Wen Shen¹, Chenjie Zhang¹, Tao Wu¹

¹Department of Cardiovascular Medicine, the Second Affiliated Hospital of Nanchang University, Nanchang, China; ²Department of Medical Technology, Jiangxi Health Vocational College, Nanchang, China; ³Department of Emergency, the Second Affiliated Hospital of Nanchang University, Nanchang, China

Contributions: (I) Conception and design: T Wu; (II) Administrative support: D Wu, H Zhou; (III) Provision of study materials or patients: T Yang, W Shen; (IV) Collection and assembly of data: X Hu, H Xiao, C Zhang; (V) Data analysis and interpretation: T Wu, D Wu, C Wang; (VI) Manuscript writing: All authors; (VII) Final approval of manuscript: All authors.

[#]These authors contributed equally to this work.

Correspondence to: Tao Wu. Department of Cardiovascular Medicine, the Second Affiliated Hospital of Nanchang University, No. 1, Minde Road, Donghu District, Nanchang, China. Email: wt47667425@163.com.

Background: It is considered that circRNA can participate in regulating the occurrence and effects of ventricular arrhythmia (VA) through competing endogenous RNA (ceRNA) mechanism, regulating pre-mRNA and regulating parental gene expression. Therefore, we used animal modeling and high-throughput differential screening to screen out circRNA related to VA and study its possible mechanism of action on VA.

Methods: The rat model of myocardial ischemia VA was established. High-throughput screening of the differentiated circRNA was conducted and verified by real-time quantitative polymerase chain reaction (qRT-PCR) and Western blot. Lv-circRNA01724 lentivirus was constructed using molecular biology. Primary isolation of the rat cardiomyocytes, hypoxia modeling, Lv-circRNA01724 transfection, mode of action verification, and dual luciferase detection of circRNA01724 and miR-323-5p was performed.

Results: Through qRT-PCR verification of circRNA01724, circRNA02230, circRNA02088, miR-323-5p, miR-330-5p, and miR-324-3p expressions, circRNA01724 was selected as the research object. Detection by Western blot showed significantly lower Cx43, ZO-1, and α -catenin expressions in rat myocardial tissue in the model group compared with the control group at 1, 7, 14, and 28 days old. On identification of the isolated primary rat cardiomyocytes by immunofluorescence, the α -SMA characteristic protein expression indicated that the isolation was successful. Verification of rat cardiomyocytes transfected with Lv-circRNA01724 suggested overexpression in cells. The miR-323-5p was also highly expressed in the rat cardiomyocyte hypoxia model following Lv-circRNA01724 transfection. Detection by flow cytometry showed that modeling of the transfected Lv-circRNA01724 had a significant increased apoptotic rate. Detection by Western blot showed that modeling of the transfected Lv-circRNA01724 cells had significantly decreased Cx43, ZO-1, and α -catenin compared with the model group.

Conclusions: High-throughput screening of circRNA01724 can promote the apoptosis of hypoxic cardiomyocytes, which is related to the rat model of myocardial ischemia VA and may be a potential target for the treatment of VA.

Keywords: High throughput screening; circular RNA (circRNA); apoptosis; myocardial ischemia; ventricular arrhythmia (VA)

Submitted Jan 12, 2022. Accepted for publication Apr 02, 2022.

doi: 10.21037/jtd-22-194

View this article at: <https://dx.doi.org/10.21037/jtd-22-194>

Introduction

Ischemic heart disease (IHD) is common cause of death in patients with cardiovascular disease and is also the primary factor that leads to heart failure. Cardiovascular risk factors continue to increase, and IHD has become the main cause of death in Western developed countries and seriously threatens human health (1). It is estimated that about 3.5 million people die from cardiovascular disease in China every year, of which more than 30% are caused by IHD. The increase in cardiovascular mortality is due to the increase in deaths from IHD (2). Myocardial ischemia refers to a pathological condition in which the blood perfusion of the heart is reduced, which leads to a decrease in oxygen supply to the heart, an abnormal energy metabolism of the myocardium, and the inability to maintain normal heart function. The direct consequence is the occurrence of angina pectoris, arrhythmia, and decreased heart function (3). There are various types of myocardial ischemia which can cause arrhythmia, most of which are ventricular arrhythmia (VA). VA is the main cause of early death in patients with myocardial infarction (MI). Among the people who survived acute MI, more than 50% still died of fatal VA (4). Therefore, research on the pathogenesis of ischemic arrhythmia is essential to improve the cure rate and develop new therapies.

The mechanism of VA is relatively complicated. VA induced by myocardial ischemia and hypoxia is closely related to the abnormal regeneration and distribution of the autonomic nerve, abnormal activity of the autonomic nerve, abnormal structure of the electrical signal conduction, and abnormal activity of the ion channels in myocardial cell membrane (5,6). Circular RNA (circRNA) is a special type of endogenous noncoding RNA (ncRNA), which exists widely and conservatively in eukaryotes. At present, research suggests that the biological mechanism of circRNA operates through competing endogenous RNA (ceRNA) by regulating pre-mRNA and regulating the expression of the parental genes (7). At the same time, the microRNA (miRNA) sponge effect of circRNA is a common phenomenon, which can regulate the expression of the miRNA. On the other hand, exon circularization can compete with classical pre-mRNA splicing to achieve a balanced state between circularization and linear splicing, which shows that circRNA can affect protein synthesis by regulating pre-mRNA splicing (8).

In this study, a rat model of myocardial ischemia VA was constructed. Using high-throughput screening of the

differentiated circRNA and their corresponding interacting miRNA, the function and possible mode of action of the circRNA at the cellular level was explored, and the possible mechanism of the circRNA on VA was expounded. We present the following article in accordance with the ARRIVE reporting checklist (available at <https://jtd.amegroups.com/article/view/10.21037/jtd-22-194/rc>).

Methods

Experimental animals and cells

Ten-week-old specific-pathogen-free (SPF) grade Sprague Dawley (SD) rats were purchased from Hunan SJA Laboratory Animal Co., Ltd., Hunan, China [license number: SCXK (Xiang) 2019-0004]. The rats were randomly divided into separate cages, raised under 22–25 °C and a standard 12-hour light-dark cycle, and allowed free access to food and water. The rat cardiomyocytes were isolated and identified from the neonatal SD rats. Animal experiments were performed under a project license (No. NCDXFLL20190506) granted by institutional committee of the Second Affiliated Hospital of Nanchang University, in compliance with the Second Affiliated Hospital of Nanchang University institutional guidelines for the care and use of animals. A protocol was prepared before the study without registration.

Experimental reagents and instruments

The following reagents and instruments were used: Invitrogen TRIzol reagent (CW0580S); Ultrapure RNA extraction kit (CW0581M); HiFiScript first-strand complementary cDNA synthesis kit (CW2569M); UltraSYBR Mixture (CW0957M), biconchonic acid (BCA) protein assay kit (CW0014S); goat anti-rabbit immunoglobulin G (IgG) cyanine (Cy)3, conjugated (CW0159S) (Beijing ComWin Biotech Co., Ltd., Beijing, China); radio immunoprecipitation assay (RIPA) lysis buffer (C1053); skimmed milk powder (P1622) (Applygen Technologies Inc., Beijing, China); bovine serum albumin (BSA) (A8020), trypsin-ethylenediamine tetraacetic acid (EDTA) solution (T1300) (Beijing Solarbio Science & Technology Co., Ltd., Beijing, China); mouse monoclonal anti-glyceraldehyde 3-phosphate dehydrogenase (GAPDH) (1/2,000) (TA-08), goat anti-mouse IgG heavy and light chains (H+L) horseradish peroxidase (HRP) conjugate (1/2,000) (ZB-2305), goat anti-rabbit IgG (H+L) HRP

conjugate (1/2,000) (ZB-2301) (ZSGB-Bio, Beijing, China); rabbit anti-connexin (Cx)43 (1/1,000) (AF0137) (Affinity, Chicago, IL, USA); rabbit anti-zonula occludens (ZO)-1 (1/1,000) (bs-1329R) (Bioss Antibodies Inc., Woburn, MA, USA); alpha-smooth muscle actin (α -SMA) (ab7817), rabbit anti- α -catenin (also known as CTNNA1) (1/5,000) (ab51032) (Abcam PLC, Cambridge, UK); Dulbecco's modified Eagle medium (DMEM) (KGM12800S-500), R1640 (KGM31800S-500); ready-to-use 4',6-diamidino-2-phenylindole (DAPI) solution (KGA215-50) (Jiangsu KeyGEN BioTECH Corp., Ltd.; Nanjing, China); fetal bovine serum (FBS) (04-001-1A) (Biological Industries, Cromwell, CT, USA); Lipofectamine[®] 3000 (18882752) (Invitrogen, Waltham, MA, USA); Annexin V-APC/7-AAD apoptosis kit (AP105-100kit) [Multisciences (Lianke) Biotech, Co., Ltd., Hangzhou, China]; dual luciferase reporter gene assay kit (RG027) (Beyotime Biotechnology, Shanghai, China); small animal ventilator (D02-DW013) (Beijing Zhongshidichuang Science and technology Development Co., Ltd., Beijing, China); illumina high-throughput sequencing system (NextSeq 500) (Illumina, Inc., San Diego, CA, USA); CO₂ incubator (BPN-80CW) (Shanghai Yiheng Technical Co., Ltd., Shanghai, China); inverted fluorescence microscope (MF53) (Guangzhou Micro-shot Technology Co., Ltd., Guangdong, China); fluorescence polymerase chain reaction (PCR) analyzer (CFX Connect™ Real-time); ultra-high sensitivity enhanced chemiluminescent imaging system (Chemi Doc™ XRS+) [Bio-Rad Laboratories (Shanghai) Co., Ltd., Shanghai, China]; high speed refrigerated centrifuge (TGL-16G) (Changzhou Zhongjie Experimental apparatus manufacturing Co., Ltd., Changzhou, China); microscope (CX41) (Olympus Corporation, Shinjuku, Tokyo, Japan); multi-mode microplate reader (S/N502000011) (Tecan Group Ltd., Männedorf, canton of Zürich, Switzerland); NovoCyte™ flow cytometer [NovoCyte 2060R, ACEA BIO (Hangzhou) Co., Ltd., Zhejiang, China]; and vertical protein electrophoresis system (DYY-6C) (Beijing Liuyi Biotechnology Co., Ltd, Beijing, China).

Animal modeling

Establishment of the rat model myocardial ischemia VA

The SD rats were raised and acclimatized to the environment for one week. An intraperitoneal (IP) injection of sodium pentobarbital (45 mg/kg) was given for anesthesia. Under aseptic condition, the rats were placed supine and fixed on the operating table. The skin was cut

along the midline of the neck, and the tissue was separated. The trachea was exposed, intubated, and connected to the ventilator. The electrocardiogram (ECG) machine was connected. The chest cavity was opened, the heart was exposed by cutting open the pericardial sac, and the upper one-third of the left coronary artery was ligated with a 6-0 circular needle with a thread. After the ECG detection confirmed that the model was successfully established, the chest cavity was sutured, and penicillin was injected intramuscularly. Twenty-four hours after modeling, tissue protection solution was added to the rat heart tissue, and the heart tissue was stored at -80 °C.

High-throughput screening of the differentially expressed circRNA

Six female SD rats were randomly allocated into two groups (n=3 rats per group). The treatments were as follows: (I) control group (Control, C), the rats were anesthetized according to the dosage for modeling, only the skin was cut, and no modeling was performed; and (II) VA model group (Model, M), the rats were modeled, and the procedure was as in "Animal modeling" above. Twenty-four hours after the modeling was completed, myocardial tissues from the two groups were taken, the total RNA was extracted, and high-throughput sequencing was performed to analyze the differential expression of the circRNA in both groups.

circRNA screening verification

Two SD female rats and one SD male rat was caged together. After the female rats became pregnant, they were raised in a single cage, and the feed was changed to growth and reproduction feed. Each pregnant rat was divided into one group, for a total of four groups. After the pregnant rat in each group had given birth, samples were obtained from the day 1, day 7, day 14, and day 28 neonatal rats (n=6 each). Myocardial tissues were taken as the control group for each of the different days. In addition, according to the method as described in "Animal modeling" above, 6 SD rats were used for modeling, and the myocardial tissues were obtained. qPCR and WB detection were performed on the model group and the 4 control groups, respectively. The experimental grouping was specifically divided as follows: (I) C (1 d), day 1 rat control group; (II) C (7 d), day 7 rat control group; (III) C (14 d), day 14 rat control group; (IV) C (28 d), day 28 rat control group; and (V) M, rat model of myocardial ischemia VA.

Table 1 Primer information

Primer name	Primer sequence (5'-3')	Primer length (bp)	Product length (bp)	Annealing temperature (°C)
circRNA01724 F	ACCCTTCCTGGATATGGTGT	20	463	57.5
circRNA01724 R	AACGGATGCTGGGCTTG	17		
circRNA02230 F	CAGGACTCCACCACTACAATCA	20	453	57.4
circRNA02230 R	GAAAGCCACAGGGAAACAAC	18		
circRNA02088 F	TAATAGTCCACCTTGTTGTCTGTC	24	351	57.3
circRNA02088 R	GCGGTTTCTTCTCCTCCAC	19		
β-actin F	GCCATGTACGTAGCCATCCA	20	375	59.5
β-actin R	GAACCGCTCATTGCCGATAG	20		
U6 F	GCTTCGGCAGCACATATACTAAAAT	25	91	61.5
U6 R	CGCTTACGAATTTGCGTGCAT	23		

Rno-miR-323-5p F: AGTGGTCCGTGGCGGTTCCGC; Rno-miR-324-3P F: CCACTGCCCCAGGTGCTGCTGG; Rno-miR-330-5P F: TCTCTGGGCCTGTGTCTTAGGC. Downstream primers: universal primers of Beijing ComWin Biotech Co., Ltd., Beijing, China.

Fluorescent quantitative PCR

After RNA was extracted, cDNA was synthesized according to the reverse transcription kit. Using cDNA as the template, real-time fluorescent quantitative PCR was used to detect the relative expression levels of circRNA and miRNA in the tissues of each group. The primer sequences were as shown in *Table 1*.

Western blot

Lysis solution was added to each group of tissues (or cells), which were then placed on ice for 30 minutes and centrifuged at 4 °C 10,000 rpm for 10 minutes. The supernatant was carefully aspirated for total protein. The protein concentration was determined according to the BCA kit. The protein was denatured, the sample was loaded, and sodium dodecyl sulfate (SDS) gel electrophoresis was performed for 1–2 hours, followed by wet transfer for 30–50 minutes. Incubation with the primary antibodies was performed at 4 °C overnight, followed by the secondary antibody at room temperature (RT) for 1–2 hours. Enhanced chemiluminescence (ECL) solution was added dropwise onto the membrane and exposed in the gel imaging system. The gray value of each antibody band was analyzed with “Quantity one” software.

Primary isolation and identification of the rat cardiomyocytes

The neonatal SD rats were sterilized with 75% alcohol

for 1–3 minutes, and the heart was quickly removed under aseptic condition and placed in the precooled phosphate buffer saline (PBS) to remove the residual blood vessels and fascia on the surface. It was washed repeatedly to remove the residual blood. The area near the apex below the coronary sulcus was cut. The myocardial tissue was cut into small pieces of 0.5–1 mm³ and let stand, and the supernatant was discarded. Then, 0.1% trypsin with three times its volume was added and digested for 10 minutes, blow with a pipette gun and mix evenly, and naturally sedimented. The supernatant was discarded, and an appropriate amount of digestive solution was added (0.1% type II collagenase + 0.1% trypsin) and digested in a water bath at 37 °C for 10 minutes. During this period, the myocardial fragments were kept in suspension by vortex oscillation, blow with a pipette gun and mix evenly gently 2–3 times, and naturally sedimented. The upper suspension was transferred to the complete medium to terminate digestion. Digestive solution was added to the remaining myocardial fragments, and tissue digestion was repeated. The supernatant was collected and digested 3–4 times until tissue whitening was achieved. At the last collection, the digestion was terminated, and all supernatant was combined and centrifuged at 400 g for 8 minutes. The supernatant was discarded, and the culture medium was added for resuspension. After filtration with a 40-μM mesh, the cell density was adjusted, and the differential was cultured in the culture flask for 30 minutes. The adherent cells used were fibroblasts. The non-adherent cardiomyocytes were collected for further culture and passage.

Immunofluorescence identification

The culture dish with cells crawling (Cell crawling, which means that the slide is allowed to immerse in the cell culture medium and the cells grow on the slide) was obtained, washed with PBS, and fixed with 4% paraformaldehyde for 15 minutes. Then, this was soaked in PBS and permeated with 0.5% Triton X-100 (prepared in PBS) at RT for 20 minutes. BSA (concentration 5% in sterile water) was added dropwise and blocked at 37 °C for 30 minutes. A sufficient amount of diluted primary antibody α -SMA (1:200) was added dropwise and incubated overnight at 4 °C. Then, diluted fluorescent secondary antibody Cy3 (1:200) was added dropwise and incubated at 37 °C for 30 minutes. This was then soaked in PBS, and DAPI was added dropwise and incubated in the dark for 5 minutes to undergo nuclear staining. This was washed with PBS, sealed with 50% glycerol in the culture dish, and observed under the fluorescence microscope.

Construction and packaging of circRNA01724 overexpression lentiviral vector

The full sequence of circRNA01724 was searched in circBase. (EcoRI/BamHI) was cloned into the lentiviral vector pHBLV-CMV-EF1-ZsGreen-T2A-Puro and packaged (packaging was provided by Hanbio Biotechnology Co., Ltd., Shanghai, China). Transfection of the rat cardiomyocytes was carried out, and the expression effect of circRNA01724 was verified by qRT-PCR.

Hypoxia model of rat cardiomyocytes

According to the cell requirements, after the rat cardiomyocytes were transfected with circRNA01724 lentivirus, hypoxia modeling was performed and determined. The specific grouping was as follows: (I) blank control group (Control), blank cells without hypoxia modeling; (II) model group (Model), hypoxia modeling was performed; (III) lentiviral empty vector group [Lv-NC (normal control)], transfected with empty vector lentivirus, followed by hypoxia modeling; and (IV) lentiviral overexpression group (Lv-circRNA01724), transfected with lentiviral circRNA01724, followed by hypoxia modeling. After 24 hours of lentivirus transfection in groups 3 and 4, hypoxia models were established in groups 2, 3, and 4 under the condition of 95% N₂ + 5% CO₂. The medium was changed to Ca and Mg-free PBS and hypoxia was

maintained for 3 hours. After hypoxia was completed, flow cytometry detection of apoptosis was carried out, and qPCR and Western blot were conducted.

Flow cytometry detection of apoptosis

About 1×10^6 – 3×10^6 cells were collected, 1 mL PBS was added, then this was centrifuged at 1,500 rpm for 3 min and washed twice. A 5× binding buffer was diluted into a 1× binding buffer with double distilled water. The cells were resuspended with 300 μ L of precooled 1× binding buffer. Each tube had 3 μ L Annexin V-APC and 5 μ L 7-ADD added, then each was gently mixed and incubated at RT for 10 minutes in the dark. Then, 200 μ L of pre-cooled 1× binding buffer was added to each tube and mixed. Flow cytometry detection followed.

Dual luciferase detection

According to the high-throughput detection, circRNA01724 may interact with miR-323-5p. Based on the binding site information, circRNA01724-pmirGLO luciferase wild-type vector (circRNA01724wt) was constructed, and its binding site was mutated to establish the circRNA01724-pmirGLO mutant vector (circRNA01724mut). The 293T cells were transfected according to the following groups: (I) blank reagent group (Control), only the transfection reagent was added as control; (II) luciferase wild-type vector group (circRNA01724wt), only circRNA01724-pmirGLO wild-type vector was transfected; (III) luciferase wild-type vector + miRNA NC group (circRNA01724wt + NC), circRNA01724-pmirGLO wild-type vector and miRNA NC were transfected concurrently; (IV) luciferase wild type vector + miR-323-5p group (circRNA01724wt + miR-323-5p), circRNA01724-pmirGLO wild-type vector and miR-323-5p were transfected concurrently; (V) luciferase mutant vector group (circRNA01724mut), only circRNA01724-pmirGLO mutant vector was transfected; (VI) luciferase mutant vector + miRNA NC group (circRNA01724mut + NC), circRNA01724-pmirGLO mutant vector and miRNA NC were transfected concurrently; and (VII) luciferase mutant vector + miR-323-5p group (circRNA01724mut + miR-323-5p), circRNA01724-pmirGLO mutant vector and miR-323-5p was transfected concurrently. After 48 hours of transfection, the cells were collected, and 200 μ L of lysis buffer was added into each well to lyse the cells. A total of 70 μ L of lysate was obtained from each group and added to the 96-well black plate. A total of 100 μ L

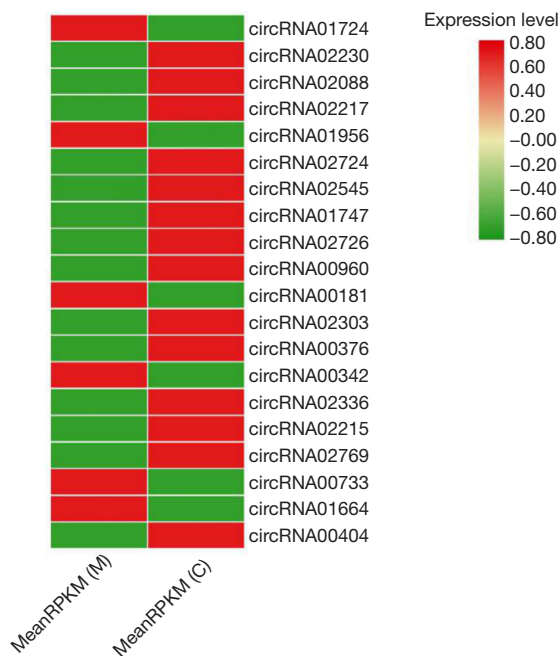


Figure 1 Heat map showing differential circRNAs. M, model group; C, normal control group. circRNA, circular RNA; RPKM, Reads Per Kilobase of transcript, per Million mapped reads.

of luciferase detection reagent was added into each well, and determination of the firefly luciferase activity was performed. Then, 100 μ L of Renilla luciferase detection reagent (detection substrate: buffer =1:100) was added into each well, and determination of the Renilla luciferase activity was conducted.

Statistical analysis

SPSS 19.0 (Statistical Product and Service Solutions 19, IBM, USA) was used to perform statistical analysis on the obtained data. The measurement data were presented as mean \pm standard deviation ($\bar{x}\pm s$). Comparison between two groups was performed with a *t*-test, and comparison between multiple groups was performed using a one-way analysis of variance (ANOVA). $P<0.05$ was considered statistically significant.

Results

High-throughput screening of circRNA

As shown in *Figure 1*, the myocardial tissues of the normal rats and myocardial ischemia VA rat model were screened

using high-throughput circRNA. The resultant heat map listed the top 20 circRNAs with the most significant differences in circRNA expression.

qPCR detection of the circRNA and miRNA expressions in rat myocardial tissue

As shown in *Figure 2*, the expression levels of circRNA01724, circRNA02230, and circRNA02088 in the C (1, 7, 14, 28 d) control group were significantly higher than those in the model group ($P<0.05$). The corresponding predictions of the respective circRNA were mutually combined. The miRNA expression levels were close to the basic trend of the circRNA, the C (1, 7, 14, 28 d) control group was higher than the model group, and the expression level of miR-323-5p in each group was relatively higher than that of miR-330-5p and miR-324-3p.

Western blot detection of the Cx43, ZO-1, and α -catenin expressions in rat myocardial tissue

As shown in *Figure 3*, the Cx43, ZO-1, and α -catenin protein expressions in the C (1, 7, 14, 28 d) control group were significantly different from those of the model group ($P<0.05$), particularly in the C (7, 14, 28 d) control group, in which the Cx43, ZO-1, and α -catenin protein expressions were significantly higher than those of the model group ($P<0.05$).

Identification of primary isolated rat cardiomyocytes

Figure 4 illustrates the immunofluorescence identification of the primary rat cardiomyocytes isolated from the neonatal SD rats. The expression of the α -SMA characteristic protein indicated that the isolation was successful.

Effect of circRNA01724 overexpression lentivirus on hypoxia modeling of rat cardiomyocytes

Figure 5A shows verification of the normal rat cardiomyocytes transfected with circRNA01724 overexpression lentivirus (Lv-circRNA01724), which indicated that Lv-circRNA01724 was overexpressed in cells after transfection. *Figure 5B* illustrates the hypoxia model of rat cardiomyocytes after Lv-circRNA01724 transfection. The results showed that after modeling of transfected Lv-circRNA01724, miR-323-5p was also highly expressed. *Figure 6* shows flow cytometry detection

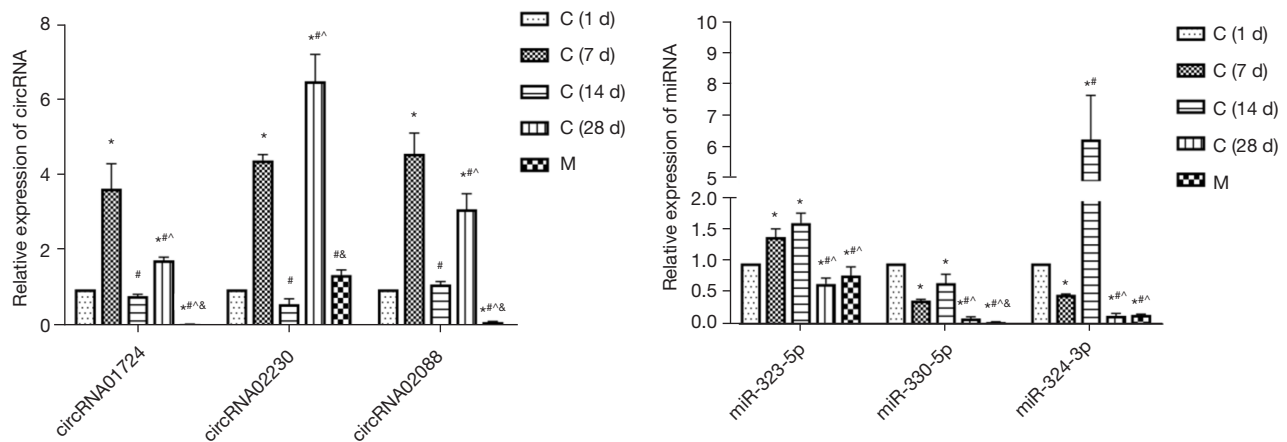


Figure 2 qRT-PCR detection of the circRNA and miRNA expressions in rat myocardial tissue. M, model group; C, normal control group, with 1, 7, 14, and 28 days as age of the neonatal Sprague Dawley (SD) rats. All data were presented as mean \pm standard deviation. Compared with C (1 d), * $P < 0.05$; compared with C (7 d), # $P < 0.05$; compared with C (14 d), ^ $P < 0.05$; compared with C (28 d), & $P < 0.05$. qRT-PCR, real-time quantitative polymerase chain reaction; circRNA, circular RNA; miRNA, microRNA.

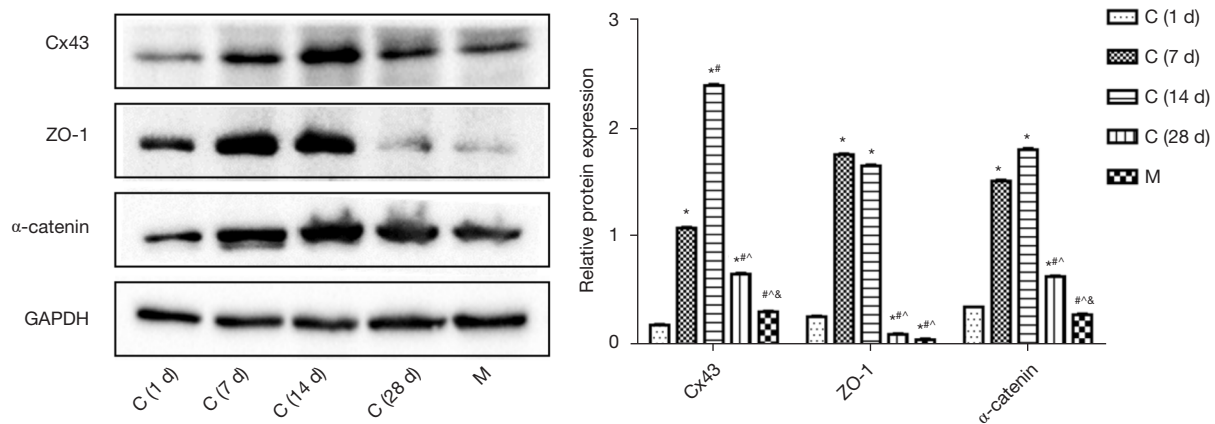


Figure 3 Western blot detection of the Cx43, ZO-1, and α -catenin expressions in rat myocardial tissue. Note: M, model group; C, normal control group, with 1, 7, 14, and 28 days as age of the neonatal Sprague Dawley (SD) rats. The data were presented as mean \pm standard deviation. Compared with C (1 d), * $P < 0.05$; compared with C (7 d), # $P < 0.05$; compared with C (14 d), ^ $P < 0.05$; compared with C (28 d), & $P < 0.05$. Cx, connexin; ZO-1, zonula occludens-1; α -catenin, alpha-catenin; GAPDH, glyceraldehyde 3-phosphate dehydrogenase.

of apoptosis in each group, and the results indicated that after modeling of transfected Lv-circRNA01724, the apoptosis rate was significantly increased ($P < 0.05$). Figure 7 shows the Cx43, ZO-1, and α -catenin protein expressions detected by Western blot after modeling of transfected Lv-circRNA01724. The results indicated that the Cx43, ZO-1, and α -catenin protein expressions were significantly decreased compared with those of the model group ($P < 0.05$ for all).

Dual luciferase verification of circRNA01724 and miR-323-5p interaction

As shown in Figure 8, the fluorescence activity of the circRNA01724 + miR-323-5p group was significantly lower than circRNA01724wt and circRNA01724wt + NC ($P < 0.05$, both), indicating that there was an interaction. After the site mutation, the circRNA01724mut + miR-323-5p group had no significant differences with circRNA01724mut

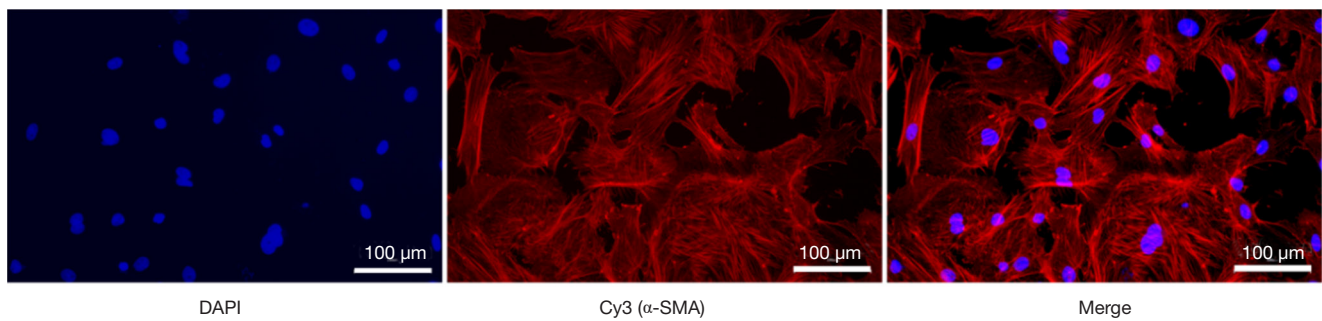


Figure 4 Immunofluorescence identification of primary rat cardiomyocytes. DAPI, 4',6-diamidino-2-phenylindole; Cy3, cyanine 3; α -SMA, alpha-smooth muscle actin.

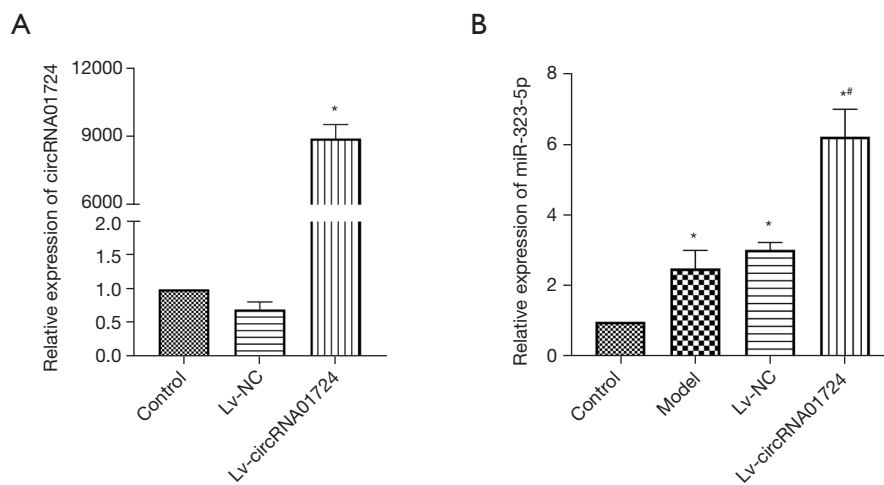


Figure 5 Effect of circRNA01724 overexpression lentivirus on hypoxia modeling of rat cardiomyocytes (A) circRNA01724 overexpression lentivirus verification (B) miR-323-5p expression after modeling of transfected Lv-circRNA01724. All data were presented as mean \pm standard deviation. Compared with the control group, * $P < 0.05$; compared with the model group, # $P < 0.05$. NC, normal control; Lv-NC, lentiviral empty vector group.

and circRNA01724mut + NC ($P > 0.05$), indicating that circRNA01724 had an interaction with miR-323-5p.

Discussion

In the pathogenesis of MI, myocardial cell necrosis caused by ischemia is a key factor that causes myocardial cell apoptosis (9). In recent years, some research on circRNA has made significant progress in the study of the disease. A study has reported that ciRS-7 can act as a sponge for miR-7 (10). The target genes for miR-7 are PARP and SP1 pro-apoptotic genes. Therefore, ciRS-7 can cause cardiomyocyte damage and accelerate the process of MI. In this study, we constructed the rat VA model by surgical

modeling, and verified the success of the model by detecting the electrocardiogram of rats. The differentially expressed circRNA01724 was screened by high-throughput and verified by qPCR with low expression in the myocardial ischemia VA model. In order to verify its function, through hypoxia modeling of the rat cardiomyocytes, and transfection of circRNA01724 overexpression lentivirus (Lv-circRNA01724), it was found that Lv-circRNA01724 could promote apoptosis, and significantly downregulated Cx43, ZO-1, and α -catenin expressions. The interaction between circRNA01724 and miR-323-5p was confirmed by dual luciferase assay.

Cx remodeling (including expression changes, redistribution, or abnormal combination) can cause

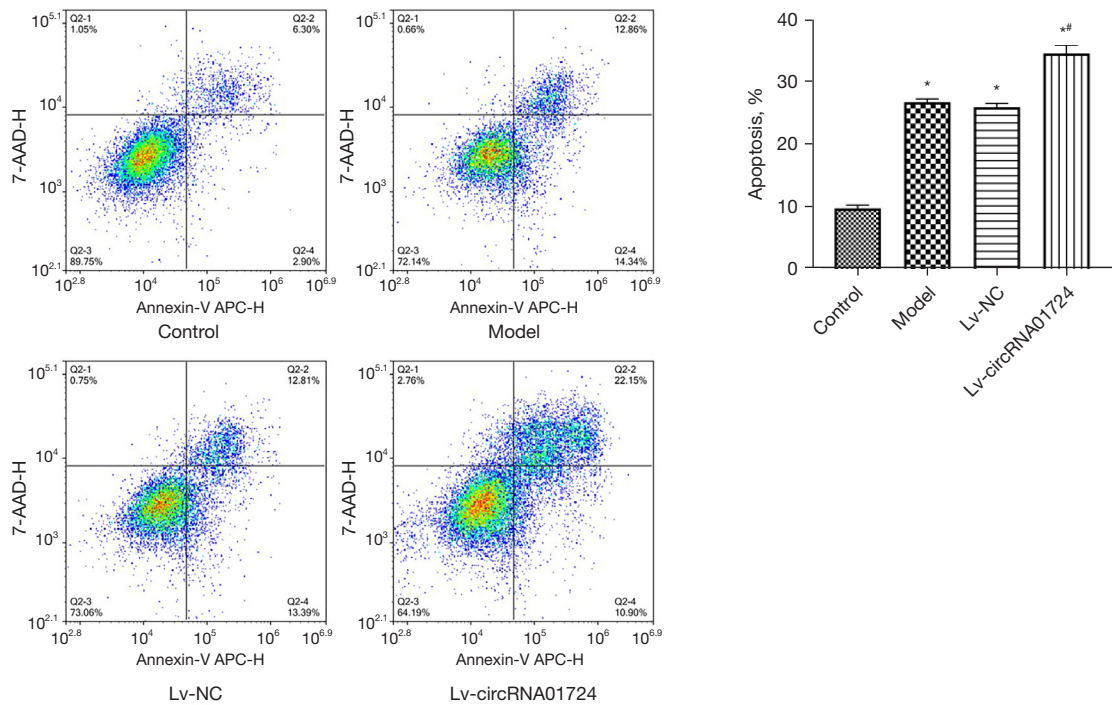


Figure 6 Flow cytometry detection of apoptosis after transfection with *Lv-circRNA01724*. The data were presented as mean ± standard deviation. Compared with the control group, * $P < 0.05$; compared with the model group, # $P < 0.05$. *Lv-NC*, lentiviral empty vector group.

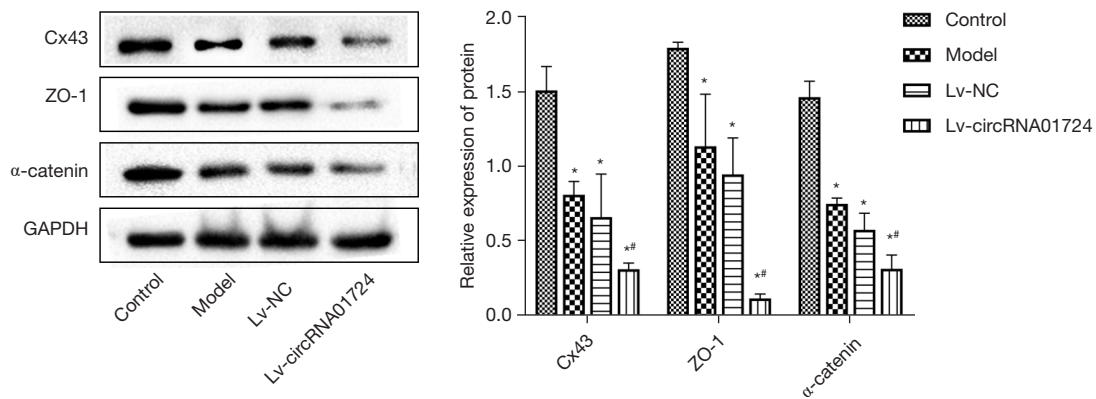


Figure 7 Western blot detection of Cx43, ZO-1, and α -catenin expressions after modeling of transfected *Lv-circRNA01724*. The data were presented as mean ± standard deviation. Compared with the control group, * $P < 0.05$; compared with the model group, # $P < 0.05$. Cx, connexin; ZO-1, zonula occludens-1; α -catenin, alpha-catenin; GAPDH, glyceraldehyde 3-phosphate dehydrogenase. *Lv-NC*, lentiviral empty vector group.

abnormal communication of the cardiomyocytes, thereby inducing arrhythmia (11). Cx43 is the most important channel protein expressed in the cardiac working cells. The decrease of its expression and phosphorylation levels and

its abnormal distribution can reduce the cardiac conduction rate and lead to arrhythmia (12). Down-regulation of the Cx43 expression by 90% can decrease the electrical conduction velocity of the heart by 50%, and down-

```

circRNA01724wt 5'-3'  CGACGUGUCACAGACCACCUUGC
miR-323-5p 3'-5'  CGCUUGCGCGGUGCCUGGUGGA
circRNA01724mut 5'-3'  CGACGUGUCACACAUCAACAUGC

```

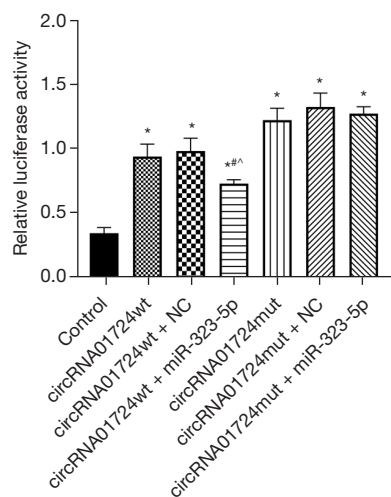


Figure 8 Dual luciferase detection of circRNA01724 and miR-323-5p interaction. All data were presented as mean \pm standard deviation. Compared with control, * $P < 0.05$; compared with circRNA01724wt, # $P < 0.05$; compared with circRNA01724wt + NC, ^ $P < 0.05$. NC, normal control.

regulation of the Cx43 expression by 50%, in addition to slowing down the conduction velocity, can also cause a large amount of electrical coupling and uncoupling, leading to VA (13). ZO-1 is a protein associated with the tight junction (TJ), which is related to the maintenance and regulation of the epithelial fence and barrier function. It is also involved in the regulation of cell material transport, maintenance of epithelial polarity, cell proliferation and differentiation, tumor cell metastasis, and other important processes (14). Since the structure and function of ZO-1 are closely related to other members of the tight junctions, in most cases, as long as ZO-1 is damaged, the functions of the tight junctions will change accordingly, therefore ZO-1 is often used as an index to observe the barrier and permeability functions of the tight junction in various tissues (15). α -catenin is a cytoskeletal protein, which has multiple sites of action and can interact with other protein molecules to perform its functions (16). In the cytoplasm, β -catenin and γ -catenin directly bind to the intracellular part of E-cadherin. α -catenin then binds to β -catenin and γ -catenin and connects it to the actin of the cytoskeleton to perform its role (17).

According to the experimental results, the expressions

of Cx43, ZO-1, and α -catenin were decreased after VA modeling. This indicates that myocardial cells were damaged and lost their normal functions. Lv-circRNA01724 transfection further aggravated the damage of cardiomyocytes and led to increased apoptosis. This indicated that up-regulation of circRNA01724 could lead to apoptosis of the hypoxic cardiomyocytes. The results of dual luciferase showed that circRNA01724 might also exert its function by acting as a miRNA sponge.

In conclusion, this study showed that the high-throughput screening of circRNA01724 has a pro-apoptotic effect on hypoxic cardiomyocytes and is related to the myocardial ischemia VA model. It may be a potential target, and its specific mechanism of action needs further in-depth study.

Acknowledgments

Funding: This study was supported by the National Natural Science Foundation of China (grant No. 81860068).

Footnote

Reporting Checklist: The authors have completed the ARRIVE reporting checklist. Available at <https://jtd.amegroups.com/article/view/10.21037/jtd-22-194/rc>

Data Sharing Statement: Available at <https://jtd.amegroups.com/article/view/10.21037/jtd-22-194/dss>

Conflicts of Interest: All authors have completed the ICMJE uniform disclosure form (available at <https://jtd.amegroups.com/article/view/10.21037/jtd-22-194/coif>). The authors have no conflicts of interest to declare.

Ethical Statement: The authors are accountable for all aspects of the work in ensuring that questions related to the accuracy or integrity of any part of the work are appropriately investigated and resolved. Animal experiments were performed under a project license (No. NCDXFLL20190506) granted by institutional committee of the Second Affiliated Hospital of Nanchang University, in compliance with the Second Affiliated Hospital of Nanchang University institutional guidelines for the care and use of animals.

Open Access Statement: This is an Open Access article distributed in accordance with the Creative Commons Attribution-NonCommercial-NoDerivs 4.0 International

License (CC BY-NC-ND 4.0), which permits the non-commercial replication and distribution of the article with the strict proviso that no changes or edits are made and the original work is properly cited (including links to both the formal publication through the relevant DOI and the license). See: <https://creativecommons.org/licenses/by-nc-nd/4.0/>.

References

- Mendis S, Davis S, Norrving B. Organizational update: the world health organization global status report on noncommunicable diseases 2014; one more landmark step in the combat against stroke and vascular disease. *Stroke* 2015;46:e121-2.
- Abdel-Kawy HS. Chronic pantoprazole administration and ischemia--reperfusion arrhythmias in vivo in rats--antiarrhythmic or arrhythmogenic? *Cardiovasc Ther* 2015;33:27-34.
- Cain ME. Impact of denervated myocardium on improving risk stratification for sudden cardiac death. *Trans Am Clin Climatol Assoc* 2014;125:141-53; discussion 153.
- Del Rio CL, Dawson TA, Clymer BD, et al. Effects of acute vagal nerve stimulation on the early passive electrical changes induced by myocardial ischaemia in dogs: heart rate-mediated attenuation. *Exp Physiol* 2008;93:931-44.
- Knollmann BC, Roden DM. A genetic framework for improving arrhythmia therapy. *Nature* 2008;451:929-36.
- Hoogaars WM, Engel A, Brons JF, et al. Tbx3 controls the sinoatrial node gene program and imposes pacemaker function on the atria. *Genes Dev* 2007;21:1098-112.
- Salzman J, Gawad C, Wang PL, et al. Circular RNAs are the predominant transcript isoform from hundreds of human genes in diverse cell types. *PLoS One* 2012;7:e30733.
- Zhang XO, Wang HB, Zhang Y, et al. Complementary sequence-mediated exon circularization. *Cell* 2014;159:134-47.
- Orogo AM, Gustafsson ÅB. Cell death in the myocardium: my heart won't go on. *IUBMB Life* 2013;65:651-6.
- Geng HH, Li R, Su YM, et al. The Circular RNA Cdr1as Promotes Myocardial Infarction by Mediating the Regulation of miR-7a on Its Target Genes Expression. *PLoS One* 2016;11:e0151753.
- Riquelme MA, Kar R, Gu S, et al. Antibodies targeting extracellular domain of connexins for studies of hemichannels. *Neuropharmacology* 2013;75:525-32.
- Chen F, Zhao WT, Chen FX, et al. High glucose promotes gap junctional communication in cultured neonatal cardiac fibroblasts via AMPK activation. *Mol Biol (Mosk)* 2014;48:687-95.
- Liu D, Zhou H, Wu J, et al. Infection by Cx43 adenovirus increased chemotherapy sensitivity in human gastric cancer BGC-823 cells: not involving in induction of cell apoptosis. *Gene* 2015;574:217-24.
- Wu J, Zhou XJ, Sun X, et al. RBM38 is involved in TGF- β -induced epithelial-to-mesenchymal transition by stabilising zonula occludens-1 mRNA in breast cancer. *Br J Cancer* 2017;117:675-84.
- Steelant B, Farré R, Wawrzyniak P, et al. Impaired barrier function in patients with house dust mite-induced allergic rhinitis is accompanied by decreased occludin and zonula occludens-1 expression. *J Allergy Clin Immunol* 2016;137:1043-1053.e5.
- Sonam S, Vigouroux C, Jégou A, et al. Direct measurement of near-nano-Newton forces developed by self-organizing actomyosin fibers bound α -catenin. *Biol Cell* 2021;113:441-9.
- Le S, Yu M, Yan J. Phosphorylation Reduces the Mechanical Stability of the α -Catenin/ β -Catenin Complex. *Angew Chem Int Ed Engl* 2019;58:18663-9.

(English Language Editor: C. Mullens)

Cite this article as: Hu X, Wu D, Zou B, Xiao H, Yang T, Wang C, Zhou H, Shen W, Zhang C, Wu T. Effect of high-throughput screening of circRNA01724 on a rat model of myocardial ischemia ventricular arrhythmia. *J Thorac Dis* 2022;14(4):1172-1182. doi: 10.21037/jtd-22-194